International Journal of Thermophysics, Vol. 16, No. 4, 1995

Measurements of the Relative Permittivity of Liquid Water at Frequencies in the Range of 0.1 to 10 kHz and at Temperatures Between 273.1 and 373.2 K at Ambient Pressure

D. P. Fernández,[1,2] A. R. H. Goodwin,[1,3] and J. M. H. Levelt Sengers[1,4]

Received September 28, 1994

The static relative permittivity (dielectric constant) of water has been determined from capacitance measurements at frequencies between 0.1 and 10 kHz, in the temperature range from 273.2 to 373.2 K at ambient pressure. The capacitor used for these measurements was formed from sapphire-insulated concentric cylinders. The specific conductance of the water used was maintained within 20% of the lowest value ever observed, which is better than in all previous experiments in this range. The new data shed some light on a discrepancy between sets of literature data in liquid water between the triple and boiling points.

KEY WORDS: audiofrequency measurements; coaxial-cylinder capacitor; electrical conductivity; electrode-polarization correction; static dielectric constant; sample purification; water.

1. INTRODUCTION

Recently, we compiled and evaluated a database for the zero-frequency (static) relative permittivity (dielectric constant) of water and steam [1]. In the range of maximum practical importance, namely, in liquid water from

[1] Thermophysics Division, National Institute of Standards and Technology, Gaithersburg, Maryland 20899, U.S.A.

[2] Permanent address: Departamento Química de Reactores, Comisión Nacional de Energía Atómica, 1429 Buenos Aires, Argentina.

[3] Present address: Center for Applied Thermodynamic Studies, University of Idaho, Moscow, Idaho 83843, U.S.A.

[4] To whom correspondence should be addressed.

0195-928X/95/0700-0929$07.50/0

the triple point to the boiling point at ambient pressures, discrepancies exist between two groups of data sets that lead to appreciable uncertainty in the temperature derivative of the dielectric constant in this range. The resolution of the discrepancy was the motivation for the present work. We report new measurements of the dielectric constant of water in this range, with particular attention paid to cell stability, water purity, and the elucidation of instrumental effects.

In the temperature range from 273 to 373 K in liquid water there are nine sources of high-quality data [2–12]. These data were obtained by either of two experimental techniques, capacitance measurements [2, 3, 6–12] or resonance techniques [4, 5], each with quite different sources of systematic error. For details the reader is referred to Ref. 1 and the original work cited therein.

In Fig. 1, we compare the various data sets, using a fit to the data of Malmberg and Maryott [2] as the reference, simply because these data appear to be the most precise and extensive. The nine independent data sets fall essentially into two groups that differ systematically; the group defined by the data of Malmberg and Maryott [2] and those of Dunn and

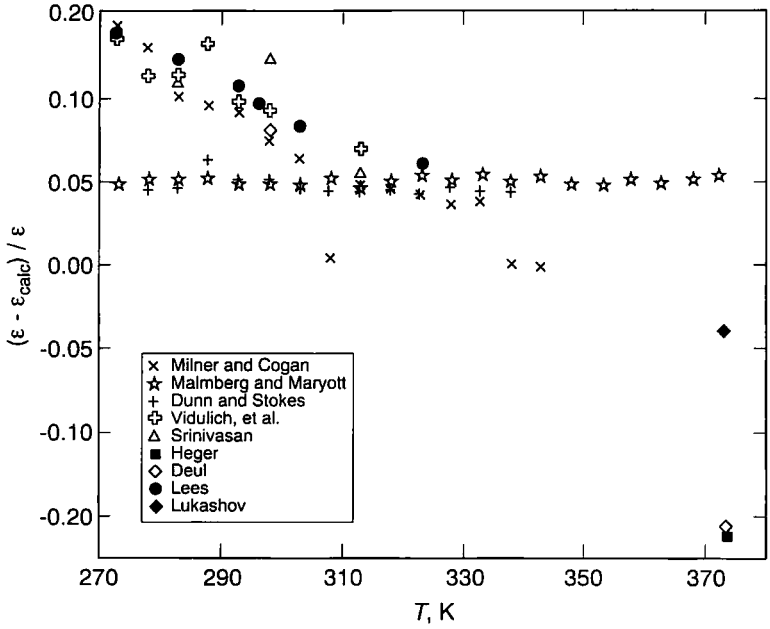

Fig. 1. Deviation $\Delta\varepsilon = \varepsilon - \varepsilon_{calc}$ of the dielectric constant $\varepsilon(T, p = 0.1\ \text{MPa}, H_2O)$ with ε_{calc} from a fit to the data of Malmberg and Maryott [2]. × [4, 5]; ☆ [2]; + [3]; ✣ [6, 7]; △ [8]; ■ [9]; ◇ [10]; ◆ [12]. Ref. 1 contains all these data, corrected to the ITS-90 temperature scale.

Stokes [3] fall below the other data at temperatures from 273 to 320 K, and above them at the higher temperatures, leading to an uncertainty in the derivative of the dielectric constant, ε, with respect to temperature $(\partial\varepsilon/\partial T)_p$ of approximately 1%. The data of Malmberg and Maryott [2] are in excellent agreement with the values reported by Dunn and Stokes [3]. Malmberg and Maryott obtained their values of the static dielectric constant from capacitance measurements at frequencies from 3 to 96 kHz [2], and Dunn and Stokes did similarly, at frequencies from 10 to 520 kHz [3]. As we discuss in more detail, however, the purity of the water samples used by Malmberg and Maryott and by Dunn and Stokes was not as high as that of many of the other data sources.

Capacitance measurements at audio frequencies are quite sensitive to the conductance of the sample. To make this point, we plot, in Fig. 2, the capacitance measured by us as a function of the inverse frequency at 298.15 K for two samples of different conductivity. The sample with the low conductance represents the best purity we have been able to obtain, approximately 20% above the pure-water limit. The other sample has a conductance higher by about a factor of 5. The significant parts of Fig. 2 are the behavior at low frequencies (right-hand side) and the behavior near the minimum of the capacitance, at around 5 kHz. At frequencies exceeding 5 kHz, near the abscissa, the particular instrument used, described in Section 2.1, quickly loses precision, and the steep rise in capacitance observed there is probably within the uncertainty of the measurement. The most striking feature in Fig. 2 is the increase in the measured capacitance of the impure sample, compared to that of the pure one, at low frequency (right-hand side), by as much as 5% for $f = 0.1$ kHz. A more subtle, but more ominous effect, however, is the decrease in the measured capacitance of the impure sample, relative to the pure one, at the high-frequency end of the usable range, by about 0.1% at $f = 5$ kHz. Qualitatively similar behavior was found at 373 K. The first effect is well characterized, and due to electrode polarization, discussed below in more detail. This is why, traditionally, capacitance data obtained at a range of audiofrequencies are extrapolated to $f \to \infty$. Here, however, is where the second effect, noted by us at 5 kHz, can lead to an erroneously low value of the dielectric constant if the purity of the sample is not optimal. That increasing electrolyte concentration leads to a lower dielectric constant is known from the work of Pottel [13], who reported dielectric relaxation in electrolyte solutions, and extracted the static permittivity from available data. The effect observed by us in samples of very low electrolyte concentration, however, is much larger than that seen by Pottel [13] and, therefore, not fully explained. The role of impurities is most serious at low temperatures, where the intrinsic conductance of water is low.

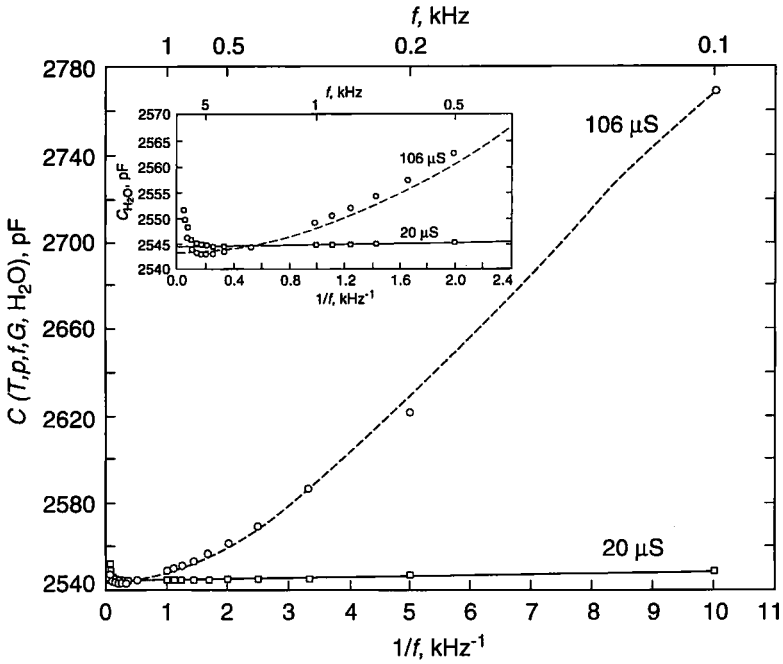

Fig. 2. Variation with inverse frequency f of the capacitance C of our cell filled with water, as determined with an *LCR* meter at $T = 298.15$ K: (□) water with conductance $G = 20\,\mu$S; (○) water with $G = 106\,\mu$S. (——) Equation (2) with coefficients adjusted to fit the data shown for water with $G = 20\,\mu$S; (-----) Eq. (2) with coefficients adjusted to fit the data shown for water with $G = 106\,\mu$S. The inset provides details for the important region $0 \leqslant f^{-1} \leqslant 2.4$.

To give an idea of the water purity of the various experimenters, we note, first, that at $T = 298$ K, the conductivity of pure water is $5.5\,\mu\text{S} \cdot \text{m}^{-1}$ [4]. Malmberg and Maryott [2], according to an estimate we made on the basis of the information provided by them, used a sample with conductance of $50\,\mu\text{S} \cdot \text{m}^{-1}$, while Dunn and Stokes's [3] sample had a conductivity greater than $80\,\mu\text{S} \cdot \text{m}^{-1}$. The other data sets in Fig. 1 appear to be less precise than those of [2]. The data sets obtained in the audiofrequency range from 0.1 to 10 kHz, however, were carried out on samples with a much higher water purity than that of Ref. 2, while in the experiments carried out at higher frequencies the impurity effects are less significant. Thus the audiofrequency data reported by Vidulich et al. [7] at 298.15 K were obtained for a water sample with a conductivity of $7\,\mu\text{S} \cdot \text{m}^{-1}$, and those of Srinivasan [8] for a sample with a conductivity of $10\,\mu\text{S} \cdot \text{m}^{-1}$. Vidulich and Kay [6] discussed the effect of conductivity on capacity measurements, and its dependence on frequency, and drew attention to the high purity of their own sample compared to that of Malmberg and

Maryott [2]. Rusche [15], whose values, mostly in the supercooled region, are not shown in Fig. 1, used water with a conductivity of $15\,\mu S \cdot m^{-1}$, only about three times the lowest observed value. The remaining data sets in Fig. 1 had a lower water purity, but the data were taken at higher frequencies than the experiments mentioned above, typically from 10 kHz to several megahertz. Milner [4] and Cogan [5] (who both used the same apparatus), and Lees [11], reported a conductivity of $150\,\mu S \cdot m^{-1}$. Heger [9], as well as Deul and Franck [10] used water with significant impurities, quoting upper bounds of $2000\,\mu S \cdot m^{-1}$ at 298.15 K [9] and $10{,}000\,\mu S \cdot m^{-1}$ at 373.15 K [10], respectively. For further details, see Ref. 1.

For the experimental work reported here we choose to measure the capacitance of a fluid-filled concentric cylinder at frequencies between 0.1 and 10 kHz. A capacitor of this geometry was chosen because corrections for alignment are negligible and the device was, as we demonstrate, mechanically stable. Our design is close to that described by Younglove and Straty [16]. This design was also used by others, for example, to determine the dielectric constant of liquid hydrocarbons [17, 18].

Prior to commencing the present measurements we were aware of three sources of dispersion: (i) electrode polarization, (ii) ionic atmosphere relaxation, and (iii) dielectric relaxation. The magnitudes of these items depend on the ionic concentration. We describe each error source in turn.

The term electrode polarization refers to the nonuniform distribution of solutes in the fluid surrounding the capacitance electrodes. It is responsible for the universally observed increase of the capacitance of water-filled cells when the frequency decreases. See, for instance, Fig. 2 (right-hand side) and Refs. 2, 6–8, and 15. There is a variety of phenomena occurring near the electrodes that are dependent on the amplitude and frequency of the applied voltage [19]. In our case the potential difference between the electrochemically inert metallic electrodes is about 0.1 V and Faradaic processes are negligible; this corresponds to an ideally polarizable electrode, in which no exchange of electrons occurs between the solution and electrode. In these circumstances the only effect of the electric field is to change the charge density at the metallic surface. That is, the ions migrate in an electric field. At low frequency these ions have sufficient time to reach the surface of the electrodes in large numbers and thus add an impedance to the system. This is called double-layer capacitance and is considered responsible for the increase in capacitance with decreasing frequency. Any model for the double-layer capacitance must describe the behavior in the vicinity of the electrode as well as the decay into the bulk fluid (diffuse layer). The former is extremely dependent on the properties of the surface, especially its ability to adsorb the ions present in solution, and is consequently difficult to predict. Several workers have proposed quantitative

models to describe the frequency behavior in the bulk fluid. For example, the theory reported by Buck [20] indicates that the diffuse layer relaxation may occur at a few kilohertz and has an f^{-2} frequency dependence.

In an applied field, the counterion charge cloud around a given ion becomes asymmetric. The mobility of the ion is decreased because of the opposite motion of the counterions and their solvated water molecules. This effect lowers the fluid conductivity. At higher frequencies, when the period of the applied field is shorter than the dielectric relaxation time of the ionic atmosphere, the asymmetry of the atmosphere disappears and the conductivity rises, lowering the dielectric constant. The frequency dependence for the dielectric constant of an electrolyte solution due to the ionic atmosphere has been modeled, with the result that the relaxation time of the ionic atmosphere for pure water at 298 K corresponds to frequencies of about 1 MHz, far exceeding the audiofrequency range used by us [21].

Finally, we mention dielectric relaxation, which describes the decay of the molecular polarization during the reorientation of the dipoles in an applied oscillating electric field. At sufficiently high frequencies, the dipoles do not have time to equilibrate during the period of an ocillation. The dielectric relaxation time is about 8.27 ps at 298.15 K [22]. Dielectric relaxation becomes a significant source of uncertainty only at frequencies in the GHz range. At $f = 1$ GHz, for instance, the real component of the permittivity is 0.5% below the static value. It is clear that dielectric relaxation is of no concern in the experiments discussed in this paper.

2. EXPERIMENTS

2.1. Apparatus

The concentric-cylinder capacitor is shown in Fig. 3; it was fashioned after that described by Younglove and Straty [16]. The two concentric cyclinders and central conical support were each machined from 316 stainless steel and electropolished. Each cylinder was insulated from the central post by six 1-mm-diameter sapphire spheres, three of them located at each end. The vacuum capacitance between the plates was about 33 pF. The assembled capacitor was attached to the end closure of a stainless-steel cylindrical pressure vessel, in which the capacitor was suspended. The containment vessel and conical support formed the third terminal in the capacitance measurement. This vessel was sealed with a gold o-ring. The electrical feedthroughs consisted of the center conductor of stainless-steel coaxial cable, a polytetrafluoroethane ferrule, and a compression nut brazed to the outer sheath of the coaxial cable. This cable had an air dielectric and PTFE disk spacers and it continued unbroken out of the

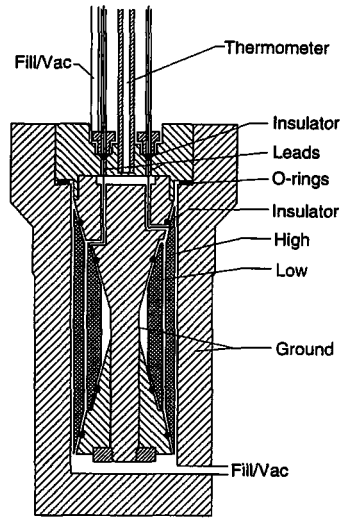

Fig. 3. Cross section through the concentric-cylinder capacitor. Sapphire spheres were used to insulate the two electropolished stainless-steel cylinders from the grounded conical support. The vessel was sealed with a gold o-ring and electrical feedthroughs were constructed from PTFE and stainless steel. An industrial-grade platinum resistance thermometer protruded into the fluid-filled cavity. The assembled device was suspended inside a stirred-fluid thermostat.

thermostat fluid. An industrial-grade 100-Ω platinum resistance thermometer, which was sealed into the vessel lid with a compression fitting, was in direct contact with the fluid. It was used solely to monitor the stability of the temperature within the cell.

The assembled vessel was placed in a stirred fluid, which was an equal mole fraction mixture of 1,2-ethanediol and water, thermostat controlled to better than 3 mK. The temperature of the bath fluid was measured with a long-stem platinum resistance thermometer, which was checked frequently at the triple point of water and was reported on the ITS-90 temperature scale [23]. The temperature was determined from resistance measurements by means of a ratio bridge. The thermometer's sensing element was located in a plane which passed through the center of the capacitor and was about 0.3 m below the thermostat's fluid–air interface. The sample temperature

was inferred from that of the thermostat fluid. For the liquid–water dielectric-constant measurements at 298 K where $d\varepsilon/dT \approx -0.36\ \mathrm{K}^{-1}$, an uncertainty not exceeding 0.15 K in the temperature will generate less than 0.05% uncertainty in the dielectric constant. In view of the excellent thermostat stability and the low uncertainty of our thermometry, we conclude that inferring sample temperature from the thermostat fluid value should not have introduced a significant systematic error into our measurements.

Three devices were used to determine the capacitance of the cell: (a) an automatic transformer bridge Model CGA-78, which was based on the General Radio 1615A and operated at frequencies between 0.1 and 10 kHz; (b) an Andeen–Hagerling bridge Model 2500A, which operated solely at a frequency of 1 kHz; and (c) a GenRad *LCR* meter, which operated at about 200 discrete frequencies between 0.1 and 100 kHz.[5] Items b and c were calibrated by the manufacturers prior to use. The precision of the capacitance C obtained from each device depended on the fluid conductivity, frequency, and capacitance. According to information supplied by the manufacturers, in the best case, devices a and b could provide values of C with a precision of 0.0005%, while device c had a precision of about 0.02%. We used all three devices to determine the vacuum capacitance but did not use b for most measurements with water, because of its single operating frequency; it was used at 1 kHz to check the values obtained from the other two devices.

Pressures between 0.2 and 0.4 MPa were measured with a strain-gauge pressure transducer, which, when calibrated against an air-lubricated deadweight gauge, was found to have an uncertainty of 0.1%. Since for water $(\partial\varepsilon/\partial p)_T \approx 0.04\ \mathrm{MPa}^{-1}$, use of this pressure gauge should not introduce an uncertainty in the dielectric constant greater than 0.004%. Measurements were corrected to a pressure of 0.1 MPa, by means of values for $(\partial\varepsilon/\partial p)_T$ obtained from the correlation of Archer and Wang [24].

2.2. Sample Purity

Preliminary measurements of the water-filled cell capacitance indicated that variations in the fluid conductivity G introduced a significant systematic error. At 298 K, and a frequency of 10 kHz, we estimated from the inset of Fig. 2 that $(\partial G/\partial C)_{P,T} \approx -0.02\ \mathrm{pF}\cdot\mu\mathrm{S}^{-1}$, while at 1 kHz $(\partial G/\partial C)_{P,T} \approx +0.04\ \mathrm{pF}\cdot\mu\mathrm{S}^{-1}$. Hence, it is of paramount importance to

[5] To describe materials and experimental procedures adequately, it is occasionally necessary to identify commercial products by the manufacturer's name or label. In no instance does such identification imply endorsement by the National Institute of Standards and Technology, nor does it imply that the particular product or equipment is necessarily the best available for the purpose.

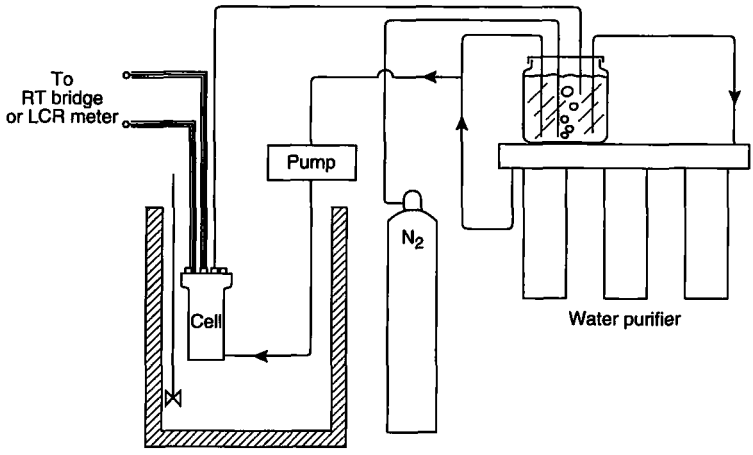

Fig. 4. Schematic for the water purification apparatus. Fresh distilled water flowed from a plastic container, where CO_2 was displaced by N_2, through an E-pure ion-exchange column, into a chromatographic pump, required to create a pressurized fluid, on through the cell and back into the reservoir. All interconnecting tubing and valves were stainless steel.

maintain the water purity at the highest possible level. In our work we adopted the following procedure to maintain the fluid at the lowest possible conductivity, with the equipment shown schematically in Fig. 4. First, a sample of distilled water was placed in a Nalgene (see footnote 5) plastic container, and dissolved CO_2 was then displaced by passing nitrogen through the sample. The water was then passed into the "E-pure" water purification system supplied by Barnstead Inc. (see footnote 5). It was capable of providing water at a temperature of 298 K with a conductivity of $5.5\,\mu S \cdot m^{-1}$, which equals the value obtained from the correlation by Marshall [14]. The water circulated from the storage vessel through the purifier and back into the feed tank until the fluid had reached the expected conductance. It was then ready to be pumped into the cell.

2.3. Procedure

The cell components were thoroughly washed in the following fluids before assembly and use: (a) a 1% HNO_3 aqueous solution at a temperature of 350 K, (b) propanone with a mole fraction purity of better than 0.999, and (c) distilled water at 373 K.

In addition to the procedures described above, we list the typical sequence of operations required to obtain the capacitance of the water-filled cell under precisely defined conditions: (a) The cell was evacuated for

Table I. Capacitance of the Concentric Cylinder Filled with Water Extrapolated to Infinite Frequency $C_\infty = C(T, p = 0.1\ \text{MPa}, f \to \infty, H_2O)$ and Under Vacuum $C_v = C(T, p = 0)$, Static Dielectric Constant ε, Conductance G, and Conductivity κ at Temperature T for Liquid Water[a]

Index	T (K)	C_∞ (pF)	U_{C_∞} (pF)	C_v (pF)	ε	U_ε	G (μS)	κ ($\mu S \cdot m^{-1}$)
LCR01	273.174	2850.50	0.20	32.434	87.88_3	0.03_3	4.59	1.25
LCR02	283.142	2725.58	0.18	32.441	84.01_4	0.01_5	9.55	2.61
LCR03	293.143	2603.51	0.10	32.446	80.23_9	0.01_1	16.9	4.61
LCR05	298.139	2544.10	0.12	32.449	78.40_1	0.01_0	21.4	5.84
LCR06	298.154	2544.48	0.08	32.448	78.41_4	0.01_0	20.7	5.65
LCR07	303.132	2486.91	0.15	32.452	76.631	0.009	28.7	7.83
LCR08	313.125	2377.07	0.08	32.457	73.235	0.009	44.3	12.1
LCR10	323.129	2270.64	0.12	32.462	69.94_6	0.01_1	67.0	18.3
LCR11	323.139	2270.24	0.08	32.461	69.93_4	0.01_1	63.4	17.3
LCR13	343.127	2072.75	0.40	32.473	63.82_7	0.01_4	146	39.8
LCR14	343.134	2071.62	0.38	32.472	63.79_0	0.01_4	127	34.6
LCR15	343.147	2072.08	0.16	32.472	63.80_6	0.01_4	126	34.5
LCR17	353.128	1979.68	0.38	32.479	60.94_6	0.01_8	176	48.0
LCR18	353.130	1978.70	0.28	32.479	60.91_9	0.01_8	179	48.8
LCR19	353.154	1977.48	0.42	32.479	60.87_8	0.01_8	170	46.5
LCR21	363.137	1888.77	0.22	32.485	58.13_7	0.02_9	225	61.3
LCR23	373.113	1803.57	1.86	32.493	55.50_3	0.04_9	305	83.1
LCR24	373.147	1803.96	1.20	32.491	55.51_5	0.04_9	298	81.2
TB01	273.174	2850.30	0.06	32.434	87.87_7	0.01_5	4.59	1.25
TB02	283.142	2725.07	0.14	32.441	83.99_8	0.01_0	9.55	2.61
TB03	293.143	2603.09	0.12	32.446	80.226	0.009	16.9	4.61
TB04	298.138	2556.11	0.08	32.606	78.388	0.008	21.5	5.84
TB05	298.139	2544.11	0.03	32.449	78.401	0.008	21.4	5.84
TB06	298.154	2544.18	0.14	32.448	78.406	0.008	20.7	5.65
TB07	303.132	2487.02	0.18	32.451	76.637	0.007	28.7	7.83
TB08	313.125	2376.48	0.24	32.457	73.216	0.009	44.3	12.1
TB09	313.131	2387.97	0.13	32.613	73.195	0.009	44.7	12.1
TB10	323.129	2270.74	0.13	32.463	69.94_6	0.01_2	67.0	18.3
TB11	323.139	2270.81	0.16	32.461	69.95_2	0.01_2	63.4	17.3
TB12	333.120	2179.31	0.32	32.624	66.79_0	0.01_5	97.6	26.5
TB13	343.127	2073.92	1.24	32.474	63.86_1	0.02_0	146	39.8
TB14	343.134	2971.79	0.52	32.472	63.79_7	0.02_0	127	34.6
TB15	343.147	2072.39	0.42	32.472	63.81_7	0.02_0	126	34.5
TB16	353.121	1990.10	0.48	32.636	60.96_8	0.03_2	182	49.4
TB17	353.128	1982.61	0.74	32.479	61.03_9	0.03_2	176	48.0
TB18	353.130	1983.60	1.46	32.479	61.07_0	0.03_2	179	48.8
TB19	353.154	1979.83	0.62	32.479	60.95_2	0.03_2	170	46.5
TB20	363.127	1894.52	2.06	32.485	58.31_7	0.05_2	235	64.1
TB21	363.137	1893.55	2.54	32.485	58.28_6	0.05_2	225	61.3
TB22	373.111	1819.35	1.08	32.650	55.71_8	0.08_0	325	88.1
TB23	373.113	1813.53	2.00	32.493	55.80_8	0.08_0	305	83.1
TB24	373.147	1810.52	2.46	32.491	55.72_0	0.08_0	298	81.2

[a] Uncertainties U_{C_∞} and U_ε are reported as 2 standard deviations. See text for details.

about 12 h, until the pressure in the pumping line was below 0.3 Pa at the required temperature; (b) the vacuum capacitance was measured at the required temperature; (c) the cell was filled with water, from the purifier described above, to a pressure of about 0.15 MPa; (d) the purge valve was then opened and water allowed to flow through the cell, usually for 2 days but not less than 12 h, until the conductivity had reached a minimum; (e) the flow was shut off, and the cell sealed and then connected to a vacuum pump to degas the sample; (f) water was again allowed to flow into the cell until the pressure reached about 0.15 MPa and the degassing process was repeated; (g) the pressure in the cell was increased, with a chromatographic pump, until it reached the value required for the measurements; (h) the capacitance was measured as a function of frequency with both instruments; (i) the water was removed by purging with nitrogen gas, and the cell evacuated to a pressure less than 0.4 Pa; and (j) the vacuum capacitance was measured again. The procedure was repeated at each temperature.

In total, successful measurements of the capacitance of the water-filled cell were performd for 24 samples. For many of these samples, both transformer-bridge (TB) and *LCR* meter (LCR) results are available. For each instrument, we report the results, discussed in the next section, in Table I, in ascending order of temperature, labeling each result by the instrument used and by the sample number. Thus, the symbols TB05 and LCR05 refer to the identical sample but different instruments.

3. RESULTS AND ANALYSIS

3.1. Vacuum Capacitance

Prior to commencing the measurements with water we assembled the cell and determined the vacuum capacitance $C_V = C(T, p = 0)$, required to calculate the dielectric constant ε as a function of temperature. We used all three capacitance instruments discussed above in Section 2.1 and found, at any one temperature, that the capacitance values measured with the two high-precision devices (a) and (b) differed fractionally by less than 5×10^{-6}. After one thermal excursion of about 100 K we found that the capacitance values at any temperature differed fractionally by no more than 1×10^{-5}.

The vacuum capacitance, about 32 pF, determined before and after a capacitance measurement of the water-filled cell never differed by more than $2 \cdot 10^{-5}$ over the 3 h needed to determined the capacitance of the water-filled cell. The average of these two values is listed in Table I for each sample. We took the value of 0.0005 pF as an estimate of the standard deviation of the value of the vacuum capacitance.

The linear thermal expansion coefficient, obtained from capacitance measurements at 10 temperatures, agrees to 1% with the literature value for type 316L stainless steel [25].

3.2. Capacitance and Conductance of the Water-Filled Cell

Values of capacitance $C'(T, p, f, H_2O)$ and conductance G were obtained from measurements of the complex impedance of the water-filled capacitor, by means of two of the instruments described earlier, namely, the transformer bridge (TB) and the *LCR* meter (LCR). The frequencies used with the transformer bridge were 0.1, 0.3162, 1, 3.162, and 10 kHz. For the *LCR* meter we used about 15 frequencies in the range from 0.1 to 10 kHz.

The measured conductances did not appear to have any appreciable frequency dependence. They were converted to values of conductivity κ by means of the relationship $\kappa = G\varepsilon_0/C(T, p=0)$. Our values of κ so determined are shown in Fig. 5 as deviations from the values reported in Ref. 14. At all temperatures our values of the specific conductivity were no more than 20% above the accepted value for pure water [14].

After equilibration for a time of at least 300 s, the measured capacitance of the cell filled with liquid water at 298 K changed less than 0.005% in 1 h (which corresponds to a conductivity change of less than

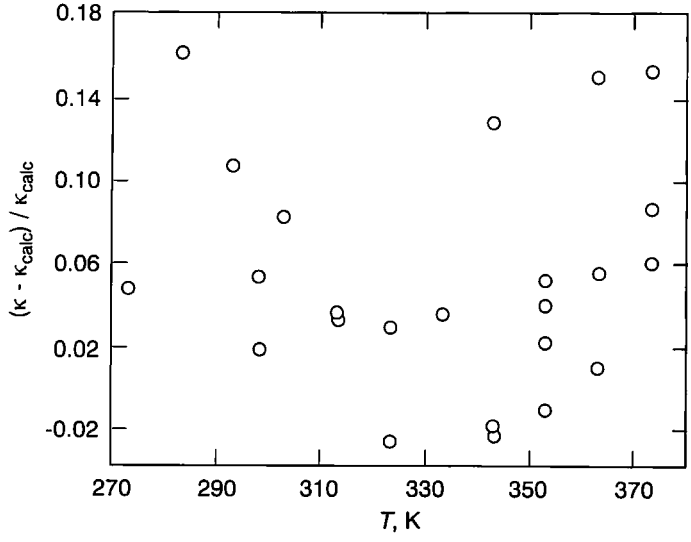

Fig. 5. Fractional deviations $\Delta\kappa/\kappa = \{\kappa - \kappa_{calc}\}/\kappa$ of the conductivity κ of the fluid in the cell from the correlation by Marshall [14].

0.3% per h) at a frequency of 1 kHz. At 373 K the capacitance changed by 0.02% per h and the conductivity by 2% per h, again at 1 kHz.

We also determined the change in the capacitance reading for the water-filled cell as a function of sine-wave excitation amplitude. At 333 K, with a fluid of conductance of 100 μS, the capacitance values obtained from the *LCR* meter changed by less than 0.005% when the amplitude was increased from 0.5 to 1.3 V a.c. at 1 kHz; this change leads to negligible error. For the same experimental conditions, the capacitances obtained from the transformer bridge varied noticeably when the voltage was varied over the range from 0.03 to 1.5 V a.c. The actual change of measured capacitance over this voltage range had a nonuniform dependence on frequency: It was 0.03% at 10 kHz, 0.01% at 3.2 kHz, 0.06% at 1 kHz, and 0.18% at 0.3 kHz. In actual experiment with the transformer bridge the excitation voltage is set automatically and is therefore not a controlled parameter. Since the dielectric constant values that we report are determined by the high-frequency capacitance data, the observed variations for the transformer bridge are marginally significant at worst, and they are considered in the data analysis as a source of random error.

3.3 Correction for Effect of Conductance on Instrument Performance

As a check on the performance of each instrument, we compared the values of capacitance obtained from each device with that of a model circuit shown in Fig. 6. It was constructed from two standard capacitors, denoted C_1 and C_2, each with a capacitance of (1000.001 ± 0.001) pF, in parallel with a low-inductance metal film resistor. The resistance of each metal film resistor was measured with a Hewlett Packard multimeter with a fractional resolution and reproducibility of better than 5×10^{-5}. The resistance was chosen such that the conductance G of the resistor was within 10% of the value corresponding to the conductance of the water-filled cell at each temperature.

We found that the *LCR* meter was able to reproduce the values of capacitance and conductance of the model circuit over the entire temperature, conductance, and frequency range encountered in our experiment, and the maximum value for the quantity $(C_M - C_1 - C_2)$ did not exceed 0.5 pF.

For the transformer bridge, however, the measured capacitance C_M at a selected conductance did not equal $C_1 + C_2$, or 2000 pF. As Fig. 7 shows for the case of this bridge, the difference between the measured capacitance and $C_1 + C_2$ was as large as 100 pF at 0.1 kHz, but only 13 pF at 10 kHz, at the highest conductance shown, 300 μS, which is typical of that of the water-filled cell at the normal boiling point. At lower conductances, the

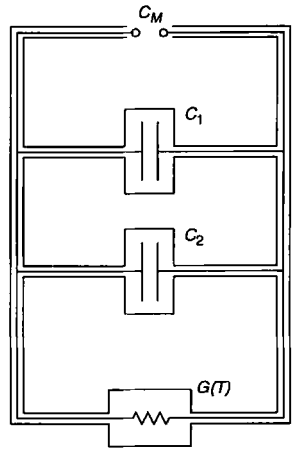

Fig. 6. Schematic of the equivalent circuit used to determine the variation in measured capacitance C_M with frequency. The conductance $G(T)$ is chosen to represent the conductance of the water-filled cell at the experimental temperatures. The two standard, air-dielectric, capacitors each have a capacitance C_i, where for $i=1$ and 2, $C_i=(1000.001\pm0.001)$ pF.

residual capacitance $(C_M-C_1-C_2)$ decreased, irregularly but reproducibly varying as a function of temperature, to reach 1 pF at 273 K. We found that $(C_M-C_1-C_2)$ was independent of the value of the standard capacitor between 0 and 200 pF; this supports the conclusion that this uncertainty arises because the bridge assigns a parallel capacitance to the resistance in order to establish the balance condition. We assumed that the transformer bridge performed identically when determining the capacitance of a water-filled cell of the same conductance and used the differences shown in Fig. 7 to correct the experimental values measured with the transformer bridge.

In some cases, the difference between the model circuit conductance and that of the water-filled cell was as large as 10%. Consequently, the quantity $(C_M-C_1-C_2)$ could not be determined with negligible uncertainty; this results in another source of random error in capacitance measurements with the transformer bridge. In the absence, however, of any better calibration for this instrument, we corrected the values of C obtained

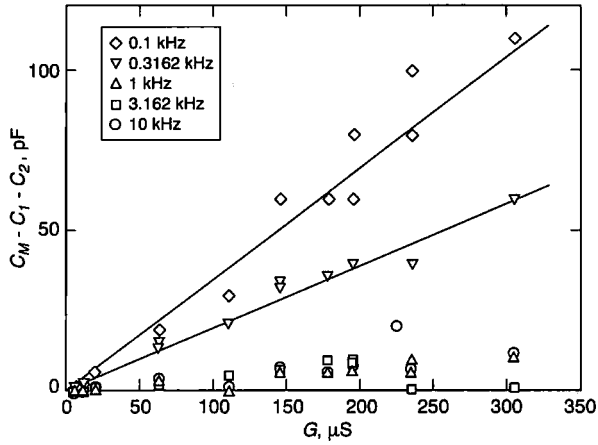

Fig. 7. Values of $(C_M - C_1 - C_2)$ for the transformer bridge determined at conductance G values between 0 and 303 μS typical of the conductance of a water-filled cell at experimental temperatures from 273.15 to 373.15 K. The lines are guides to the eye, marking the results for the lowest two frequencies.

when the cell was filled with water assuming that the following relationship held:

$$C(T, p, f, H_2O) = C'(T, p, f, H_2O) - \{C_M(f, G(T)) - C_1 - C_2\} \quad (1)$$

with $C'(T, p, f, H_2O)$ the measured value, $C(T, p, f, H_2O)$ the corrected value, and $C_M(f, G(T))$ the bridge reading of the model circuit at a conductance G representative of that of the water-filled cell at temperature T.

We likewise corrected the readings of the *LCR* meter by means of Eq. (1), but as mentioned before, these corrections never exceeded 0.5 pF.

3.4. Toward an Estimate of the Variance of the Capacitance Measurements

The variance of the capacitance of the water-filled cell at a given frequency, for a sample at given pressure and temperature, if not a priori known, could in principle be obtained from many repeat measurements. In our case, we know the variance induced by the uncertainties in pressure and temperature measurements; it is negligible for all practical purposes. We also know to some extent the variance of the correction of the capacitance reading that we obtain from the calibration by means of the model circuit, as described in the pevious section. The major contribution to the variance, however, is that due to the instrument performance during

actual measurements. This contribution cannot be estimated a priori. Only in a limited number of cases (298 and 363 K) did we have more than two repeat measurements at several frequencies. In those cases, we estimated a standard deviation as half the spread of the measurements. This crude estimate immediately revealed an important feature: The variance so estimated was roughly proportional to $1/f$. This feature is exploited in the analysis of the electrode polarization effect described next, and in subsequent uncertainty analyses.

3.5. Correction for Electrode Polarization

As discussed in Section 1, there are three effects that dominate the frequency dependence of the water-filled capacitor. Dielectric relaxation (at $f > 1$ GHz) and the electrophoretic effect (at $f > 1$ MHz) introduce insignificant uncertainty into our measurement. The third, and most significant, effect under the frequency conditions of our experiment arises from the phenomenon of double-layer capacitance (electrode polarization), which is most important at low frequency and high conductance. Figure 8 shows the variation of $C(T, p, f, H_2O)$, the capacitance of the water-filled cell corrected according to Eq. (1), as a function of inverse frequency, at frequencies between 10 and 0.1 kHz. At 298 K, where the fluid conductance is about 21 μS, the capacitance changes, as Fig. 8a shows, by about 1% over this frequency range, while at 343 K, where the conductance is about 130 μS, the same frequency range corresponds with a 15% change in $C(T, p, f, H_2O)$.

The capacitance as measured by the transformer bridge levels off at the higher frequencies. The capacitance as measured by the *LCR* meter, as mentioned in Section 1, passes through a minimum at a frequency of about 5 kHz. The increase at the higher frequencies (near the origin in Fig. 8) is an artifact indicating the rapid loss of reliability of this instrument at frequencies exceeding 10 kHz. In no case have we made use of *LCR*-meter data on the left side of the minimum in Fig. 8.

Double-layer capacitance effects may be significant for capacitance measurements at frequencies of less than 10 kHz, and increase with decreasing frequency according to an f^{-2} dependence [20]. The actual form of this frequency dependence is still a subject of controversy. In the actual corrections of experiments for this frequency dependence, any power between 0.5 and 2.0 has been used [2, 3].

In the absence of any complete model, we adopted an empirical procedure to extract the so-called infinite-frequency capacitance (a misnomer, because all our data are effectively at zero frequency), to be identified with the desired zero-frequency capacitance later, from our measured values, as

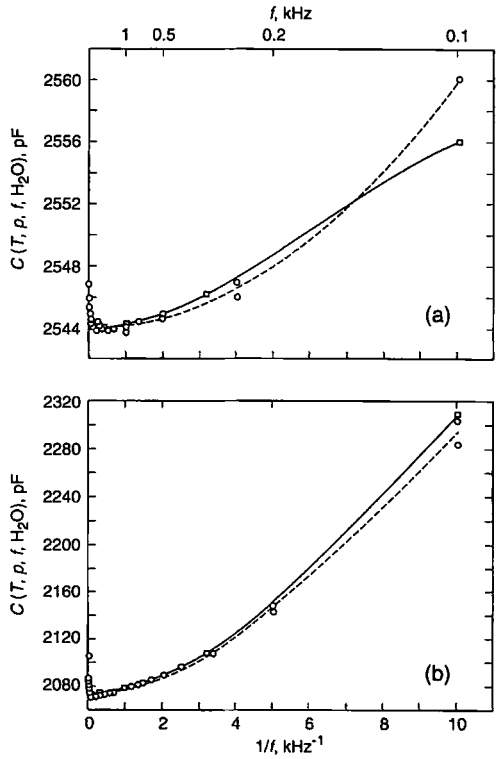

Fig. 8. The corrected capacitance $C(T, p, f, H_2O)$, Eq. (1), of the cell filled with pure water as a function of reciprocal frequency at (a) a temperature of 298.15 K and (b) a temperature of 343.15 K. Values obtained from (○) the transformer bridge, (□) the *LCR* meter, (——) Eq. (2) for the transformer bridge, and (-----) Eq. (2) for the *LCR* meter.

had previous workers [2, 3]; we used a leading correction term proportional to f^{-2}. The procedure is to extrapolate all data for the transformer bridge, or the data on the right-hand side of the minimum (cf. Fig. 8), for the *LCR* meter (all of our data are in the effective zero-frequency range characteristic of the static permittivity), to infinite frequency, to eliminate the low-frequency electrode polarization effect. Thus, for both instruments the capacitances, corrected according to Eq. (1), were fitted to the empirical function

$$C(T, p, f, H_2O) = C(T, p, f \to \infty, H_2O) + (a/f^2) + (b/f^3) \qquad (2)$$

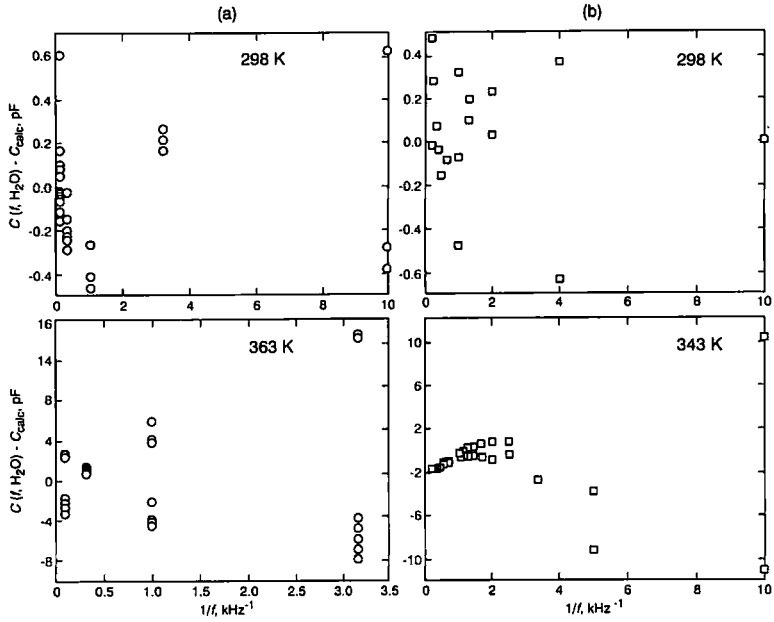

Fig. 9. The deviations of the corrected capacitance $C(T, p, f, H_2O)$ as a function of frequency from Eq. (2). (a) Transformer bridge data for sample TB04 at 298 K and for sample TB20 at 363 K. (b) *LCR*-meter data for sample LCR05 at 298 K and for sample LCR13 at 343 K.

where a and b are adjustable parameters, and $C(T, p, f \to \infty, H_2O)$, which we denote by C_∞, is the desired infinite-frequency intercept of the fit. We gave all data points a relative weight w_i proportional to the frequency; cf. Section 3.4. Analyses were performed for each instrument at each temperature. Some cases where we have a sufficient number of measurements for a given sample are shown in Fig. 9. Figure 9a represents deviations from Eq. (2) of the capacitance measurements obtained by means of the transformer bridge at 298 K for sample TB04 and at 363 K for sample TB20 in Table I. Figure 9b represents deviations from Eq. (2) for *LCR*-meter measurements at 298 K for sample LCR05 and at 343 K for sample LCR13.

We found Eq. (2) adequate for representing the data in almost all cases, except at 273 and 283 K. Here we found, for both instruments, systematic deviations of up to 0.4 pF that we could not eliminate satisfactorily by changing the functional form.

The values for the infinite-frequency intercept C_∞ are listed in Table I, separately for the transformer bridge and for the *LCR* meter.

We have tested in several cases how the value of the intercept changes if the functional form of the frequency dependence is changed. For about a dozen cases we tested the intercept value if only the first two terms in Eq. (2) are used. This is not an adequate description at any but the lowest two temperatures. Nevertheless, the intercepts so obtained differed by less than 0.01% from the values obtained with the full Eq. (2) at all but the highest temperature, 373 K. We also varied the weight assignment, for instance, by using the actual spread of the data at the higher frequencies as a measure of the variance. Although, incidentally, this made a difference, in general, the intercept did not change by more than 0.01%, compared to the one obtained by weighting with the frequency.

3.6. Calculation of the Static Dielectric Constant

As stated before, in our frequency range all data are effectively at zero frequency as far as dipole relaxation effects are concerned. To so-called infinite-frequency intercept $C(T, p, f \to \infty, H_2O)$ is no more than a mathematical device to free the low-frequency data from electrode polarization effects. We assume that $C(T, p, f \to \infty, H_2O)$ equals the zero-frequency capacitance $C(T, p, f = 0, H_2O)$ from which to determine the static dielectric constant ε. Thus we used

$$\varepsilon = \frac{C(T, p, f \to \infty, H_2O)}{C(T, p = 0)} \tag{3}$$

as the ratio of the capacitance extrapolated to infinite frequency, and the mean of the vacuum capacitance measured before and after the cell was filled with water. This analysis provided a result at a pressure of 0.2 MPa at temperatures below 333 K and at 0.4 MPa at higher temperatures. The dielectric constant was then corrected to 0.1 MPa by means of the value $(\partial\varepsilon/\partial p)_T \approx 0.044\ \text{MPa}^{-1}$ from the correlation of Archer and Wang [24]. This correction was always less than 0.03% and was made with negligible uncertainty.

In Table I we list the values of the static dielectric constant at a pressure of 0.1 MPa obtained from these analyses, along with the fluid conductance and conductivity. The data obtained with the transformer bridge and those obtained with the *LCR* meter are listed separately.

3.7. Uncertainty of the Infinite-Frequency Intercept

Each of the capacitance measurements included in the regression of Eq. (2), and also the corrections determined by the model circuit, are subject

to random variations due to various sources of error. We estimated the relative weight at each frequency (Sections 3.4 and 3.5) and use statistical means [6] to calculate the uncertainty of the intercept at infinite frequency. The estimate variance s^2 of the weighted fit of the capacitance data as function of $1/f$, Eq. (2), is defined as

$$s^2 = \sum_{i=1}^{n} \frac{w_i r_i^2}{n-k} \tag{4}$$

with r_i the residual of each of the n data points, k the number of adjustable parameters, 3 in our case, and w_i the relative weights discussed in Section 3.5. The value of s^2 was used to scale the variance of the intercept, $s'^2_{C_\infty}$, obtained from the variance–covariance matrix with relative weights, to yield the estimated standard deviation of the intercept if absolute weights had been assigned, $s_{C_\infty} = s \cdot s'_{C_\infty}$. Table I lists U_{C_∞}, which represents the uncertainty of the intercept, estimated as twice the standard deviation s_{C_∞}. To estimate the variance of the dielectric constant, Eq. (3), the variance of the vacuum capacitance (Section 3.1) needs to be added. If we compare the uncertainty so obtained (not listed in Table I, because it is not realistic) with the actual variability of dielectric constant data for different samples obtained at the same temperature, we find, perhaps not surprisingly, that the intersample differences exceed the estimated uncertainties by a factor of five or more in many cases. We use this variance, the sum of the variances of the infinite-frequency intercept and vacuum capacitance, only as a relative weight assignment in some of the further data processing.

3.8. Temperature Dependence of the Dielectric Constant, and a Final Estimate of the Uncertainty

As the last step in the analysis, the static dielectric constant data are fitted as a function of temperature. We have used a cubic in inverse temperature,

$$\varepsilon = c_0 + c_1/(T/K) + c_2/(T/K)^2 + c_3/(T/K)^3 \tag{5}$$

assigning to each data point a relative weight in accordance with the variances of the intercept, from $s_{C_\infty} = U_{C_\infty}/2$ in Table I, and from the vacuum capacitance (Section 3.1). The data for the transformer bridge and those for the *LCR* meter were fitted separately. The coefficients of each fit are listed in Table II. In the first case, the variance of the fit was 23, and in the second case, it was 30, both much larger than unity, and reaffirming that the uncertainties of the dielectric constants of the individual samples had been underestimated by a factor of about 5. Figures 10a and b show the departures of the dielectric constant data from the fitted curves for the

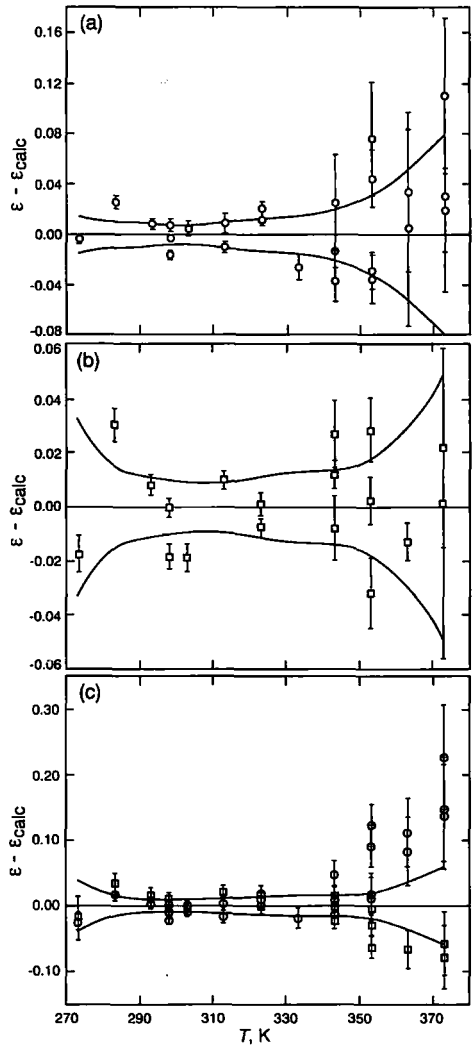

Fig. 10. Deviation $\Delta\varepsilon = \varepsilon - \varepsilon_{calc}$ of the dielectric constant ε of water from Eq. (5) fitted to our data: (○) transformer bridge; (□) *LCR* meter. Full curves indicate two standard deviations calculated on the basis of the respective fits [6]. (a) Equation (5) fitted to the transformer bridge data, with relative weights assigned on the basis of the error bars indicated; (b) Eq. (5) fitted to the *LCR*-meter data, with relative weights as before; (c) Eq. (5) fitted to the combined data set, with weights according to the variances calculated from the solid curves in a and b, respectively.

Table II. Coefficients Obtained from Eq. (5)

Coefficient	TB	LCR	TB + LCR
c_0	−41.1140	−68.5005	−59.1331
$c_1 \cdot 10^{-5}$	0.328958	0.573486	0.492117
$c_2 \cdot 10^{-7}$	0.274328	−0.451684	−0.217429
$c_3 \cdot 10^{-9}$	0.574809	0.142582	−0.081075

transformer bridge and those for the *LCR* meter, respectively. The vertical bar on each data point indicates two standard deviations, as estimated from the uncertainty of the intercept (Table I) and that of the vacuum capacitance (Section 3.1). The uncertainties of the predicted values [26] were calculated over the whole temperature range from the variance–covariance matrix and the standard deviation of the fit to Eq. (5); they do not change if all weights are multiplied by a factor. The solid curves in Fig. 10 represent two standard deviations of the predicted value. The statistical uncertainties so obtained are representative of the random scatter of the body of experimental data. These are obviously more realistic indications of the intersample variability for each instrument than the uncertainties resulting from the $1/f$ fit for individual samples. These uncertainty estimates based on the fits on Eq. (5) for each instrument, U_ε, are listed in Table I.

Finally, we repeated the fit to Eq. (5) for the two data sets combined, using the uncertainty values U_ε in Table I as a basis for relative weights. The coefficients of this combined fit are given in Table II. The variance of this fit was 12, indicating that the uncertainties used to weight the data were still somewhat underestimated. The deviations from the fitted function are displayed in Fig. 10c. The solid curves again represent two times the predicted standard deviations for the fit to the combined data. Figue 10c reveals that the data obtained with the two instruments generally agree to within combined error at temperatures up to and including 343 K. Above that temperature, the transformer bridge data depart systematically upward from the *LCR*-meter data. At 373 K, the actual spread of the dielectric constant data is about 0.3, to be compared with the value of 0.08 for two standard deviations of the transformer bridge (Fig. 10a), 0.05 for the *LCR* meter (Fig. 10b), and 0.06 for the combined fit.

3.9. Predicted Values of the Dielectric Constant and Their Uncertainty

From the coefficients of the fit to the combined data set (last column in Table II), we have calculated the dielectric constant at the nominal

Table III. Predicted Values and Statistical Uncertainties of the Dielectric Constant, Eq. (5), at Nominal Temperatures and Ambient Pressure

T(K)	ε_{calc}	U_c
273.15	87.91_1	0.04_0
293.15	80.22_0	0.01_1
298.15	78.405	0.009
303.15	76.632	0.009
313.15	73.20_5	0.01_0
323.15	69.93_0	0.01_3
333.15	66.80_0	0.01_4
343.15	63.80_7	0.01_5
353.15	60.94_3	0.02_0
363.15	58.20_0	0.03_4
373.12	55.58_1	0.05_7

experimental temperatures. These values, and the predicted uncertainties at the two-standard-deviation level, are listed in Table III. Note that the uncertainties are based on applying the principles of statistical analysis which assume Gaussian distribution of error. In view of the systematic differences between the data sets obtained with different instruments, the uncertainties in Table III should be considered to be on the low side at the high temperatures.

4. COMPARISON

The dielectric constant data at ambient pressure reported by other workers [2–12] are plotted in Fig. 11, as deviations from Eq. (5), with the coefficients from the combined fit (last column in Table III). Below 340 K, the results of Milner [4], Cogan [5], Srinivasan and Kay [8], Lees [11], and Vidulich et al. [7] are in good agreement with ours, with almost all data points reported falling within a band of -0.05 to $+0.05$ from the fitted curve, and the Lees data falling within -0.02 to $+0.01$ from this curve. At 298 K, the value reported by Deul and Franck [10] is in good agreement with the predicted curve. In the range below 340 K, the data of Malmberg and Maryott [2] and those of Dunn and Stokes [3] depart systematically from the other group of data and have a temperature slope differing by about 1%, as mentioned in Section 1.

At temperatures above 340 K, the data we obtained with different instruments no longer agree. The data obtained with the *LCR* meter follow the trend indicated by the data point of Lukashov at 373 K [12], while the data from the transformer bridge follow the trend of the Malmberg and Maryott data. At 373 K, the latter data depart from the our equation by

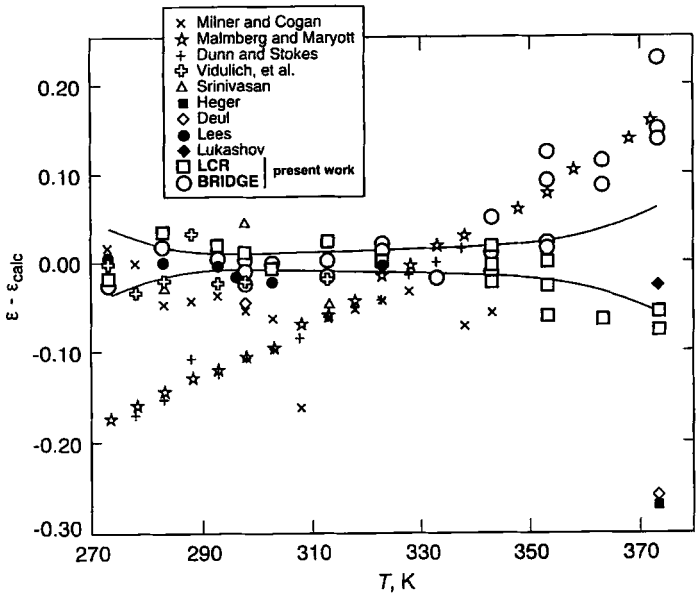

Fig. 11. Deviation $\Delta\varepsilon = \varepsilon - \varepsilon_{\text{calc}}$ of the dielectric constant ε of water from Eq. (5) fitted solely to the combined new data presented here (Fig. 10c). × [4, 5]; ☆ [2]; + [3]; ✣ [6, 7]; △ [8]; ■ [9]; ◇ [10]; ● [11]; ◆ [12]; ○, this work, transformer bridge; □, this work, *LCR* meter. Solid curves: two standard deviations as in Fig. 10c.

+0.15. The results of Heger et al. [9] and the most recent work of Deul and Franck [10], from the same laboratory, differ from our equation at 373 K by −0.27.

5. DISCUSSION

The dielectric constant data for liquid water between triple point and 340 K fall into two mutually inconsistent groups, the group of the Malmberg and Maryott [2] and Dunn and Stokes [3] data and that of all others, including new data presented here. The reasons can be understood at least partially, be it not fully.

The two main sources of error in the audiofrequency range are electrolytic contimination of the water and high intrinsic conductance of the water at the higher temperature.

The effect of electrolytic contamination, which raises the conductance, is most severe at the lower temperatures, where the intrinsic conductivity of the water is low. In the audiofrequency experiments, this lowers the capacitance in the range where the infinite-frequency extrapolation, which

eliminates the double-layer capacitance effect, is performed and, thus, leads to a dielectric constant value that is too low. Since the conductance in the Malmberg and Maryott experiment was approximately 10 times that of pure water in the range around 298 K, this explains the departure of these data from the audiofrequency experiments with higher water purity and from the higher-frequency data in the temperature range below 320 K.

That the experimental results of Dunn and Stokes [3] agree fully with those of Malmberg and Maryott [2] is a fact that defies explanation. Although the water purity was worse than that of Malmberg and Maryott, the Dunn and Stokes experiment was carried out at higher frequencies, from 10 to 520 kHz, and by means of a transformer bridge (whereas Malmberg and Maryott used a bridge without inductive elements), while attention was paid to the effect of electrolytes added, with the surprising conclusion that the results were independent of ionic concentrations, over a range high enough to bring the resistance down to a few ohms.

At the higher temperatures, on the other hand, the intrinsic conductance of water is much higher (at 373 K, the intrinsic conductivity of water is 80 times higher than at 273 K), and impurities should play a less prominent role. The principal correction to be made is associated with the low impedance of the cell, and depends on the specific bridge or meter used, as discussed in Section 3.3. Our transformer bridge readings of the capacitance in the model circuit, Fig. 6, for instance, were considerably too high when a resistance typical of the water-filled cell at 373 K was used. Malmberg and Maryott [2] state that they did not correct for this effect.

Above 320 K, our transformer bridge data remain high with respect to the *LCR*-meter data even after considerable corrections on the basis of the results for the model circuit. Also, the model-circuit measurements with the transformer bridge are ill behaved in the sense that they do not depend in a uniform way on the frequency. In contrast, the correction measured with the *LCR* meter is always smaller than 0.5 pF at any frequency and conductance in our range.

We could, in principle, not have reported the data obtained with the transformer bridge. This bridge, however, is a more precise instrument than the *LCR* meter. Also, at the lower temperatures the two instruments agree very well mutually after the still substantial correction determined with the model circuit is applied to the transformer bridge data; the data agree with most other literature data.

The transformer bridge corrections are large and more uncertain at the higher conductances. It is, of course, possible that the model circuit (Fig. 6) is not an adequate representation of the distribution of capacitive and conductive elements of the water-filled cell at the higher conductances.

If the model circuit is not adequate, however, the small size of the correction for the *LCR* meter might conceivably be an artifact as well.

For the two reasons given, innate instrument precision and model-circuit inadequacy possibly affecting both instruments, we have included both sets of data, with a lower weight for the higher-temperature transformer bridge data, in our final fit. Our data, therefore, cannot categorically exclude the results of Malmberg and Maryott above 330 K but present a strong case for the incorrectness of these data below 320 K.

ACKNOWLEDGMENTS

We gratefully acknowledge Dr. Richard F. Kayser, Chief of the NIST Thermophysics Division, for his support during the course of this project and for his critical reading of the manuscript. We are indebted to Drs. Norman Belecki, Bruce Field, and May Chung of the NIST Electricity Division, who, in addition to sharing their combined knowledge of capacitance measurements, provided the GenRad *LCR* meter and one of the nominal 1000-pF standard capacitors. We thank Dr. Vern Bean, NIST Process Measurement Division, who loaned us the CGA-78 transformer bridge. We are also indebted to Dr. Carl Andeen, of Andeen Hagerling Inc., who patiently instructed us in the operation of this bridge. We thank Dr. Yung Chi Wu, NIST Analytic Research Division, and Dr. Hugo Bianchi, Química de Reactores, CNEA, for their advice on preparation of high-purity water samples.

REFERENCES

1. D. P. Fernández, Y. Mulev, A. R. H. Goodwin, and J. M. H. Levelt Sengers, *J. Phys. Chem. Ref. Data*, in press.
2. C. G. Malmberg and A. A. Maryott, *J. Res. Natl. Bur. Std. (U.S.)* **56**:1 (1956).
3. L. A. Dunn and R. H. Stokes, *Trans. Faraday Soc.* **65**:2906 (1969).
4. C. E. Milner, Ph.D. thesis (Yale University, New Haven, CT, 1955).
5. H. L. Cogan, Ph.D. thesis (Yale University, New Haven, CT, 1958).
6. G. A. Vidulich and R. L. Kay, *J. Phys. Chem.* **66**:383 (1962).
7. G. A. Vidulich, D. F. Evans, and R. L. Kay, *J. Phys. Chem.* **71**:656 (1967).
8. K. R. Srinivasan, Ph.D. thesis (Carnegie-Mellon University, Pittsburgh, PA 1973); K. R. Srinivasan and K. L. Kay, *J. Chem. Phys.* **60**:3645 (1974).
9. H. Heger, Ph.D. thesis (University of Karlsruhe, Karlsruhe 1969); H. Heger, M. Uematsu, and E. U. Franck, *Ber. Bunsenges Phys. Chem.* **84**:758 (1980).
10. R. Deul and E. U. Franck, *Ber. Bunsenges Phys. Chem.* **95**:847 (1991).
11. W. L. Lees, Ph.D. thesis (Harvard University, Cambridge, MA 1949).
12. Yu. M. Lukashov, Ph.D. thesis (Moscow Power Institute, Moscow, 1981); Yu. M. Lukashov and V. N. Shcherbakov, *Teploenergetika* **27**(3):171 (1980).
13. R. Pottel, in *Water, a Comprehensive Treatise, Vol. V*, F. Franks, ed. (Plenum Press, New York, 1973), Chap. 8.

14. Marshall, *J. Chem. Eng. Data* **32**:221 (1989); Electrolytic Conductivity of Liquid and Dense Supercritical Water from 0°C to 800°C and Pressures up to 1000 MPa, IAPWS Guideline Statement (1990) (available from Dr. Barry Dooley, Electric Power Research Institute, 3412 Hillview Avenue, Palo Alto, CA 94304, U.S.A.).
15. E. W. Rusche, Ph.D. thesis (New Mexico University, 1966); E. W. Rusche and W. B. Good, *J. Chem. Phys.* **45**:4667 (1966).
16. B. A. Younglove and G. C. Straty, *Rev. Sci. Instrum.* **41**:1087 (1970).
17. W. M. Haynes, *Adv. Cryog. Eng.* **31**:1199 (1986).
18. C. C. Luo and R. C. Miller, *Cryogenics* **21**:85 (1981).
19. J. Braunstein and G. D. Robbins, *J. Chem. Educ.* **48**:52 (1971).
20. R. P. Buck, *J. Electroanal. Chem.* **23**:219 (1969).
21. H. S. Harned and B. B. Owen, *The Physical Chemistry of Electrolyte Solutions* (Reinhold, New York, 1950), p. 90.
22. U. Kaatze, *J. Chem. Eng. Data* **34**:371 (1989).
23. H. Preston-Thomas, *Metrologia* **27**:3 (1990).
24. D. D. Archer and P. Wang, *J. Phys. Chem. Ref. Data* **19**:371 (1990).
25. D. E. Furman, *J. Metals Trans. AIME* **188**:688 (1950).
26. M. G. Natrella, *Experimental Statistics*, *N.B.S. Handbook 91*, reprinted 1966, Superintendent of Documents, U.S. Government Printing Office.